Analysis of the Anomalous Doppler Effect from Quantum Theory to Classical Dynamics Simulations

Xinhang Xu (徐新航)[1], Jinlin Xie (谢锦林)[1]*, Jian Liu (刘健)[2], and Wandong Liu (刘万东)[1]

[1]Department of Plasma Physics and Fusion Engineering, University of Science and Technology of China, Hefei 230026, China

[2]Weihai Institute for Interdisciplinary Research, Shandong University, Weihai 264209, China

May 11, 2025

Abstract

A quantum model incorporating angular momentum conservation is developed to analyze the Normal and Anomalous Doppler Effects, demonstrating that the resonance condition is strongly influenced by the angular momentum of the wave. The resonance condition involving wave angular momentum is examined numerically, and the energy exchange ratio between the electron's parallel and gyrokinetic motion during resonance with the electromagnetic wave is simulated, exhibiting strong agreement with quantum theoretical predictions.

Keywords: Anomalous Doppler Effect, Resonant condition, Angular monmentum Conservation

PACS:

1 Introduction

The Anomalous Doppler Effect (ADE) [1–4], in which the observed frequency shift behaves contrary to the conventional Doppler Effect under specific conditions, was first theoretically predicted by Soviet physicist Vitaly L. Ginzburg [5]. This phenomenon arises when a system moves with a velocity exceeding the phase velocity of light in the medium, transferring its translational kinetic energy into internal energy while emitting radiation. A notable example, discussed by Frank in his 1958 Nobel lecture [2], shows that radiation emission does not occur through the typical transition from an excited state to a lower energy state. Instead, it proceeds from a lower to a higher energy state, powered by the system's translational kinetic energy. This counterintuitive prediction has attracted considerable attention and has inspired extensive research [6–13].

In 1967, Artsimovich [14] reported discrepancies in tokamak experiments: the electron temperature estimated from diamagnetic signals was significantly higher than that derived from electrical conductivity measurements. Although unrecognized at the time, this anomaly may represent the first experimental observation of ADE. In 1968, B. B. Kadomtsev [15] identified ADE as the underlying mechanism, in which electrons undergo

---

*Corresponding author. E-mail: jlxie@ustc.edu.cn

velocity scattering from the longitudinal to the transverse direction under resonant conditions. This process enhances the diamagnetic effect beyond what would be expected from thermal motion alone. Subsequently, a range of ADE-related phenomena have been observed, including electron beam scattering in magnetic field vacuum tubes [2], wave radiation [16–18], and runaway electron instabilities in tokamaks [19,20]. Practical applications based on ADE have also emerged, such as high-power microwave generation and runaway electron suppression in tokamaks [10,21].

The physics of the Anomalous Doppler Effect (ADE) was first elucidated through quantum analysis by Frank and Ginzburg [2,22]. In this work, we extend Ginzburg's quantum framework by incorporating the conservation of angular momentum to provide a more rigorous analysis of ADE. This approach yields new insights into the relationship between wave angular momentum and ADE under resonant conditions, which it is referred to Anomalous Doppler Resonance (ADR). For an electron moving in a magnetic field and interacting with an external electromagnetic (EM) wave, the general resonance condition is given by: $\omega = m\omega_{ce} + \vec{k} \cdot \vec{v}$, where $\vec{k}$ is the wave vector, ω_{ce} is the electron cyclotron frequency (here $\omega_{ce} > 0$), $\vec{v}$ is the electron velocity, and ω is the wave angular frequency, $m = 0, \pm 1, \pm 2, \pm 3, \ldots$ represent the Landau level [23]. Specially, for plane EM waves, we find that resonance is restricted to the fundamental harmonics ($m = \pm 1$) due to spin angular momentum conservation, reducing the condition to $\omega = \pm\omega_{ce} + \vec{k} \cdot \vec{v}$. where the negative sign refers to ADR condition while the positive sign refers to Normal Doppler Resonance (NDR) condition. This represents a significant constraint compared to previous theoretical treatments [24] which suggested possible resonance at all harmonic orders ($m = \pm 1, \pm 2, \ldots$). Despite the simplicity of the model, our analysis demonstrates that angular momentum conservation plays a crucial role in EM wave-electron resonance - an aspect that, to the best of our knowledge, has not been previously addressed in the literature.

Furthermore, we perform numerical simulations of a single electron interacting resonantly with an EM wave in the presence of uniform static electric and magnetic fields, using classical equations of motion.These simulations elucidate the relationship between wave angular momentum and the resonance mechanism. Additionally, we compute the energy transfer ratio from the electron's translational kinetic energy to its gyrokinetic energy during resonance, and the results show strong agreement with predictions from quantum theory.

The remainder of this paper is organized as follows. Section 2. develops the quantum theoretical framework incorporating angular momentum conservation. Section 3. presents our numerical approach, detailing the simulation setup, analyzing the time evolution of electron velocity and kinetic energy, investigating the resonant conditions with wave angular momentum, and examining the energy transfer ratio and polarization characteristics. Section 4. provides a comprehensive discussion of the key findings and their physical implications. Finally, Section 5. summarizes the principal conclusions and outlines potential directions for future research.

2.Quantum analysis of ADE

When a charged particle moves through a medium at a speed greater than the phase velocity of light in that medium, it induces polarization in the surrounding molecules. As these molecules return to their equilibrium state, they emit electromagnetic radiation. The constructive interference of these emissions produces the characteristic Cherenkov radiation, forming a cone-shaped wavefront as shown in Fig. 1. The direction of Cherenkov radiation is constrained to the Cherenkov radiation angle $\theta_0 = \arccos\left(\frac{c'}{v}\right)$,where c' is the speed of

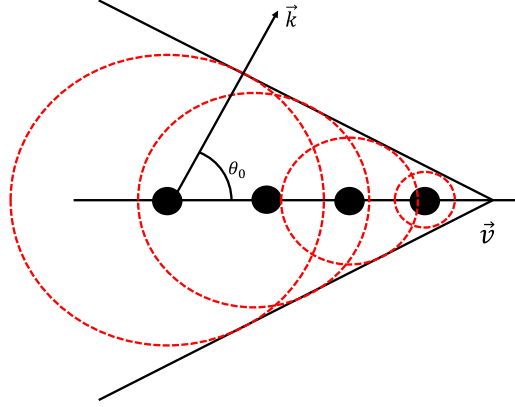light in the medium and v is the velocity of the charged particles.

Fig. 1. Schematic diagram of Cherenkov Radiation. The black points stand for the snapshot of the electron at different times, the read dash circle refers to the current radiation surface from the previous electron.

However, when the electron is replaced by a system possessing internal energy—such as an oscillator or a cyclotron electron in a magnetic field—the direction of the emitted photon is no longer determined by the interference of secondary waves and can instead occur in any direction. Considering a scenario where the system emits a photon with angular frequency ω and wavevector k, the emission process must satisfy both energy and momentum conservation:

$$
\begin{align}
T_1 + U_1 &= \hbar\omega + T_2 + U_2 \tag{1a}\\
\vec{p}_1 &= \vec{p}_2 + \hbar\vec{k} \tag{1b}
\end{align}
$$

Here the T and U represent the kinetic energy and internal energy of the system while subscripts of 1 and 2 refer to before and after emitting a photon. p represents the momentum of the system and $\hbar$ represnts reduced Planck's constant. Assuming that photon's s energy is far less than the initial kinetic energy T_1, the losses of kinetic energy after emitting a photon can be expressed as $\Delta T_{12} = T_1 - T_2 = \Delta\vec{p}\cdot\vec{v}$, where v is the velocity of the system before emitting a photon and $\Delta\vec{p} = \vec{p}_1 - \vec{p}_2 = \hbar\vec{k}$. Thus, the change of internal energy can be expressed
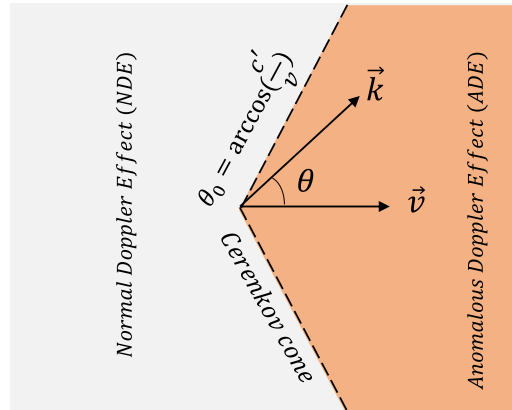

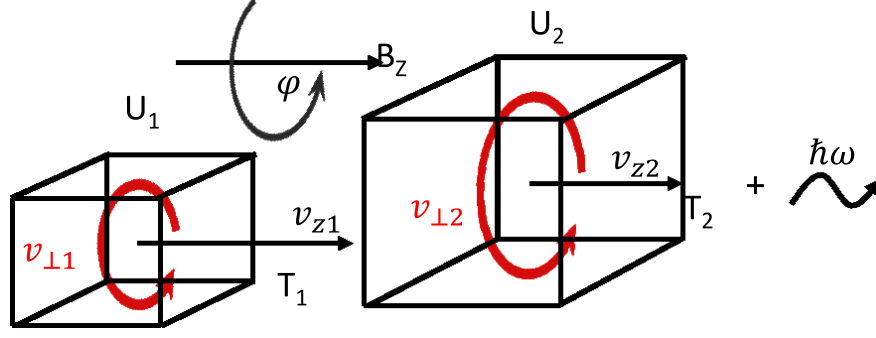Fig. 2. The region of Anomalous Doppler Effect (ADE) and Normal Doppler Effect (NDE).

Fig. 3. Schematic diagram of electron cyclotron system before and after emitting a photon. Here $U_2 > U_1, T_2 < T_1$

as

$$
\begin{aligned}
\Delta U_{21} &= \Delta T_{12} - \hbar\omega \\
&= \hbar\vec{k} \cdot \vec{v} - \hbar\omega \\
&= \hbar\omega \left(\frac{v\cos\theta}{c'} - 1 \right)
\end{aligned}
\tag{2}
$$

Here, $\omega/k = c'$, and $\Delta U_{21} = U_2 - U_1$. When the system's velocity exceeds the speed of light in the medium ($v > c'$), the sign of ΔU_{21} allows the radiation to be categorized into three distinct regions, as illustrated in Fig. 2.

1. For $\theta > \theta_0 = \arccos(c'/v)$, $\Delta U_{21} < 0$. The system produces photons by consuming its own internal and kinetic energy; this region refers to the Normal Doppler Effect (NDE).

2. For $\theta = \theta_0$, $\Delta U_{21} = 0$, the loss of kinetic energy by the system is completely converted into photon energy; this line refers to the Cerenkov Effect.

3. For $\theta < \theta_0$, $\Delta U_{21} > 0$, this region is referred to as the Anomalous Doppler Effect (ADE), where the system gains internal energy after emitting photons. It means the loss of kinetic energy is converted to photons and the system's internal energy.

In previous paper, the change of internal energy is given as $\Delta U = m\hbar\omega_{ce}$, where $m = 0, \pm 1, \pm 2, \pm 3, \ldots$ represent the Landau level, as given by V. L. Ginzburg [25], Coppi [23], Frolov [26], Frank [2], Tamm [1] and Nezlin [6]. The above content revisits the foundational work of V. L. Ginzburg [25]. In the present paper, it is further demonstrated that m actually represents the quantum number associated with the angular momentum of the emitted photon.

Let's consider the process in which an electron cyclotron system under a uniform magnetic field emits a photon along z axis, as shown in Fig. 3. The moving electron has the velocity v_z along the background magnetic field and the $v_\perp$ cyclotron velocity. The kinetic energy along z is $T = \gamma m_e c^2 - m_e c^2$, where γ refers to the Lorentz factor. The internal energy represents as $U = \frac{1}{2}\gamma m_e v_\perp^2$.

Assume the angular momentum of the system before and after emitting a photon is L_1 and L_2, respectively. The angular momentum of photon is $m\hbar$. According to the angular momentum conservation, we have

$$
L_1 = L_2 + m\hbar
\tag{3}
$$

Since the magnetic field is aligned along z direction, the angular momentum of electron along z is represented as L_z. According to the quantum theory, the electron wave in the static magnetic field can be expressed as

$$
\Psi = \Psi_0 e^{\frac{i}{\hbar}(\mathbf{p} - e\mathbf{A}) \cdot \mathbf{s}}
\tag{4}
$$

With the term Ψ_0 representing the normalized coefficient, $\mathbf{A}$ is the vector potential and $\mathbf{s}$ is the position. For a gyro-motion electron in a magnetic field, $\mathbf{s} = r\phi\,\vec{e}_\phi$, where r refers to the cyclotron radius and ϕ refers to the cyclotron angle.

The z-component of the orbital angular momentum operator can be expressed in spherical coordinates as:

$$\hat{L}_z = -i\hbar\frac{\partial}{\partial\phi} \tag{5}$$

Combining Eq. (4) with Eq. (5), we have

$$-i\hbar\frac{\partial}{\partial\phi}\Psi = (p_\phi - eA_\phi)r\Psi \tag{6}$$

As a result, the eigenvalue of L_z can be expressed as

$$L_z = (p_\phi - eA_\phi)r \tag{7}$$

With $p_\phi = \gamma m_e v_\perp$, $A_\phi = \dfrac{rB_0}{2}$, and $r = \dfrac{\gamma m_0 v_\perp}{B_0 e}$, Eq. (7) can be rewritten as:

$$L_z = \frac{1}{2}\cdot\frac{\gamma m_0 v_\perp^2}{\omega_{ce}} = \frac{U}{\omega_{ce}}, \tag{8}$$

where $\omega_{ce} = \dfrac{eB}{m_0\gamma} = \dfrac{\omega_0}{\gamma}$ and $U = \dfrac{1}{2}\gamma m_0 v_\perp^2$. Here, m_0 is the electron rest mass, γ is the Lorentz factor, and ω_0 is the electron cyclotron frequency in the rest frame (*here we choose* $\omega_0 > 0$). The conservation of angular momentum in the z-direction is expressed as

$$L_{z2} + m\hbar = L_{z1}.$$

The variation in the angular momentum of the electron along the z-axis is given by:

$$\Delta L_{21} = L_{z2} - L_{z1} = \frac{U_2 - U_1}{\omega_{ce}} = -m\hbar \tag{9}$$

Here, m is the quantum number of the photon's angular momentum in the z-direction. The internal energy change is given by $\Delta U_{21} = U_2 - U_1$. With Eq. (9), it can be transformed as:

$$\Delta U_{21} = -m\hbar\omega_{ce} \tag{10}$$

According to the Eq. (2) and Eq. (10), the change in electron energy could be presented as

$$\hbar\vec{k}\cdot\vec{v} = \hbar\omega - m\hbar\omega_{ce} \tag{11}$$

This result is consistent with previous findings [1,2,6,23,26,27]. Here, $\hbar\vec{k}\cdot\vec{v}$ represents the loss of kinetic energy ΔT_{12}, $\hbar\omega$ represents the energy of the photon, and $-m\hbar\omega_{ce}$ represents the change in the electron gyrokinetic energy ΔU_{21} (the internal energy change). The ratio between the internal energy change ΔU_{21} and the kinetic energy change ΔT_{21} can be expressed as

$$\frac{\Delta U_{21}}{\Delta T_{21}} = \frac{m\hbar\omega_{ce}}{\hbar\vec{k}\cdot\vec{v}} \tag{12}$$

This results is a critical criterion to compare with the classical dynamic simulation in the section 2. It is also proved based on classical theory in the Appendix. After simpifying the Eq. (11), we finally have the classical wave-particle resonant condition

$$\omega = k_z v_z + m\omega_{ce} \tag{13}$$

The variable *m* represents the quantum number associated with the angular momentum of the photon. Since a photon possesses both orbital angular momentum ($l\hbar$, where $l = 0, \pm 1, \pm 2, \pm 3, ...$) and intrinsic spin angular momentum ($s\hbar$, where $s = \pm 1$) [28], the total angular momentum can be expressed as $m\hbar = l\hbar + s\hbar$.

For photons carrying only spin angular momentum, two distinct quantum states are possible, characterized by the spin quantum number *m*:

1. For $m = +1$ ($\Delta U_{21} < 0$), the cyclotron electron loses internal energy upon photon emission. The emitted photon displays right-hand circular polarization . This process is known as the NDE.

2. For $m = -1$ ($\Delta U_{21} > 0$), the cyclotron electron gains internal energy through photon emission. The emitted photon exhibits left-hand circular polarization . This process corresponds to the ADE.

The above discussion described spontaneous emission phenomena of ADE and NDE without external field intervention. In our simulation model, we introduce an external plane electromagnetic (EM) wave that serves as a resonant field interacting with electrons. This plane EM wave acts as an inducing field, enabling gyro-electron to undergo stimulated absorption or emission processes. From a quantum perspective, the plane EM wave can be regarded as an ocean of photons that carry only spin angular momentum. Consequently, the same resonance conditions as those derived from quantum field theory are recovered:

- Right-hand circularly polarized waves correspond to $m = +1$ states [30], resonating only when $\omega = \omega_{ce} + \vec{k} \cdot \vec{v}$ (NDR condition)

- Left-hand circularly polarized waves correspond to $m = -1$ states, resonating only when $\omega = -\omega_{ce} + \vec{k} \cdot \vec{v}$ (ADR condition)

This exact correspondence between our classical simulation framework and quantum field theoretic predictions validates our modeling approach while providing physical insight into the angular momentum selection rules governing these resonant interactions.

Although nonlinear analyses of electron interactions with electromagnetic waves have been extensively studied [31–39], the specific role of static electric fields in these interactions has received comparatively less attention. In our approach, the uniform electric field serves a crucial function by systematically scanning the electron velocity, thereby enabling investigation across the full spectrum of resonance conditions. The inherent complexity of these nonlinear processes precludes analytical solutions, necessitating the use of numerical simulation methods to obtain meaningful physical insights.

3.Classical dynamic simulation of ADR

The ADE process has been analyzed based on quantum theory, demonstrating that the angular momentum of the emitting photon determines the resonance condition. These characteristics will be tested through the interaction of EM wave and the electron during ADR and NDR, and the energy transfer ratio can also be verified through numerical simulations.

The difference between our definition of circular polarization and the standard definition [29] stems from our choice of $\omega_0 > 0$. Here, $m > 0$ corresponds to the same rotational sense as the electron's natural right-hand gyration, which yields right-hand polarization when $\vec{k} \parallel \vec{B}_0$.
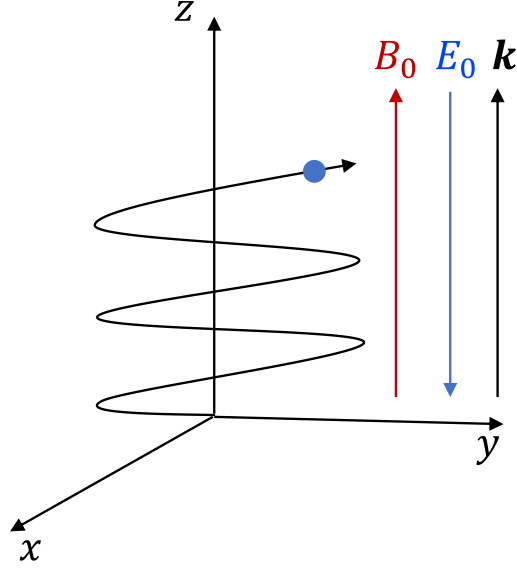
Fig. 4. The uniform static magnetic field is set along the z axis, the electrostatic field E_0 is oriented opposite to the B_0 field, and the wavevector k is aligned parallel to the B_0 field.

3.1 Numerical simulation setup

To analyze the resonant process from the perspective of classical dynamics and to provide a direct comparison between quantum and classical dynamic results, the following scenario is considered: A uniform magnetic field $\vec{B}_0$ is applied along the z-direction. An electrostatic field $\vec{E}_0$, oriented in the opposite direction to $\vec{B}_0$ (as illustrated in Fig. 4), is used to accelerate the electron. We consider the interaction between an electron entering the system with velocity v_z, parallel to the magnetic field $B_0 = B_z$, and a linearly or circularly polarized transverse electromagnetic (TEM) wave propagating in a homogeneous dielectric medium with a refractive index $n > 1$.

The induced linearly polarized wave along $\vec{B}_0$ can be decomposed into a combination of a right-hand circularly polarized wave ($m = 1$) and a left-hand circularly polarized wave ($m = -1$), such that $\vec{E}_w = \vec{E}_R + \vec{E}_L$, where $\vec{E}_R = \frac{1}{2}E_0(\vec{e}_x + i\vec{e}_y)\exp[i(\vec{k}\cdot\vec{r} - \omega t)], \vec{E}_L = \frac{1}{2}E_0(\vec{e}_x - i\vec{e}_y)\exp[i(\vec{k}\cdot\vec{r} - \omega t)]$. The magnetic field of E.M wave is

$$\vec{B}_w = \frac{\vec{k} \times \vec{E}_w}{\omega} \tag{14}$$

The six-dimensional phase space of an electron, described by its position $\boldsymbol{r}$ and momentum $\boldsymbol{p}$, are presented in the equations below. The vectors $\boldsymbol{E}$ and $\boldsymbol{B}$ represent the total field, including both static and electromagnetic components. Here, c denotes the speed of light in vacuum, e represents the electron's charge and m_0 is the electron's mass in the rest frame.

$$\frac{d\boldsymbol{r}}{dt} = \frac{\boldsymbol{p}}{\sqrt{m_0^2 + \frac{\boldsymbol{p}^2}{c^2}}},$$
$$\frac{d\boldsymbol{p}}{dt} = -e\left(\boldsymbol{E}(\boldsymbol{r},t) + \frac{\boldsymbol{p}}{\sqrt{m_0^2 + \frac{\boldsymbol{p}^2}{c^2}}} \times \boldsymbol{B}(\boldsymbol{r},t)\right) \tag{15}$$

To simulate the evolution of $\boldsymbol{r}$ and $\boldsymbol{p}$, the above system is discretized using the Volume-Preserving Algorithm. Let j denote the iteration step and $\mathrm{Cay}(\boldsymbol{A})$ represent the Cayley transform of matrix $\boldsymbol{A}$:

$$\begin{cases} \boldsymbol{r}^*_{j+\frac{1}{2}} = \boldsymbol{r}^*_j + \dfrac{\Delta t^*}{2\gamma_j}\boldsymbol{p}^*_j, \\[2mm] \boldsymbol{p}^{*-} = \boldsymbol{p}^*_j + \dfrac{\Delta t^*}{2}\boldsymbol{E}^*_{j+\frac{1}{2}}, \\[2mm] \boldsymbol{p}^{*+} = \mathrm{Cay}\left(\dfrac{\Delta t^* \hat{\boldsymbol{B}}^*}{2\gamma^{*-}}\right)\boldsymbol{p}^{*-}, \\[2mm] \boldsymbol{p}^*_{j+1} = \boldsymbol{p}^{*+} + \dfrac{\Delta t^*}{2}\boldsymbol{E}^*_{j+\frac{1}{2}}, \\[2mm] \boldsymbol{r}^*_{j+1} = \boldsymbol{r}^*_{j+\frac{1}{2}} + \dfrac{\Delta t^*}{2\gamma_{j+1}}\boldsymbol{p}^*_{j+1}, \end{cases} \tag{16}$$

The dimensionless parameters are momentum $p^* = p/(m_0 c)$, magnetic field $B^* = B/(e\tau_{ce}m_0)$, total electric field $E^* = E/(\frac{m_0 c}{\tau_{ce}e})$, time step $\Delta t^* = \Delta t/\tau_{ce}$, and position $r^* = r/(\tau_{ce}c)$ respectively, where the τ_{ce} is the electron cyclotron period ($\tau_{ce} = 2\pi/\omega_{ce}$) and $\gamma^* = \sqrt{1 + p^{*2}}$ is Lorentz factor. The dimensionless magnetic matrix $\mathbf{B}^*$ [40] is written as

$$\hat{B}^* = \begin{pmatrix} 0 & B^*_z & -B^*_y \\ -B^*_z & 0 & B^*_x \\ B^*_y & -B^*_x & 0 \end{pmatrix} \tag{17}$$

To illustrate the system evolution, the parameters are set as following: background magnetic field $B_0 = 0.02\,T$, wave angular frequency $\omega_s = 1.5\omega_0$ where $\omega_0 = (eB_0)/m_0$, wavevector $\vec{k} = 10^5/\mathrm{m}$, the electric field component of the electromagnetic wave $E_w = 9\,\mathrm{V/m}$. The propagation of induced wave with linear polarization is parallel to z axis, and the electrostatic field is $E_0 = -2.5\,\mathrm{V}$. The time resolution is always chosen to satisfy $\Delta t = \min\left(\frac{2\pi}{50(\vec{k}\cdot\vec{v})}, \frac{2\pi}{50\omega_0}, \frac{2\pi}{(50\omega_0)}\right)$ to ensure the accuracy of the simulation.

The evolution of the electron's motion is shown in Fig. 5. As the electron accelerates from stationary in the electrostatic field (Fig. 5(b)), the resonant frequencies increase simultaneously (Fig. 5(a)). The change of parallel velocity caused by electromagnetic wave can be quantified as $\Delta v = v_z - v_{zE0}$ as shown in Fig. 5(c), where v_z represents the parallel velocity under the given scenario, while v_{zE0} denotes the parallel velocity resulting solely from the electrostatic field, which can be calculated using a theoretical equation as

$$v_{zE0} = \frac{eE_0 t}{m_0\sqrt{1 + \left(\frac{eE_0 t}{m_0 c}\right)^2}} \tag{18}$$

The cyclotron velocity is shown in Fig. 5(d). The work done by electromagnetic wave is shown in fig. 5(e), which can be calculated by integrating the power with time as $E_{\|\mathrm{emw}} = \int P_{\|\mathrm{emw}} dt$, and $P_{\|\mathrm{emw}} = -e\vec{v}_\perp \times \vec{B}_{\perp\mathrm{emw}} \cdot v_z$. Since all discrete data points are available from the simulation, it is not difficult to integrate all the discrete data over time. Fig. 5(f) shows the gyro-kinetic energy evolution with time, where $E_\perp = \frac{1}{2}m_e v_\perp^2$.

3.2.Validation of energy transfer ratio

As shown in Fig. 5(a), around $23\tau_{ce}$, the normal doppler frequency matches that of the induced wave, leading to a rapid increase in the cyclotron velocity $v_\perp$ (Fig. 5(b)). Simultaneously, the change in parallel velocity induced by the electromagnetic wave also increases. This phenomenon can be interpreted as the electron
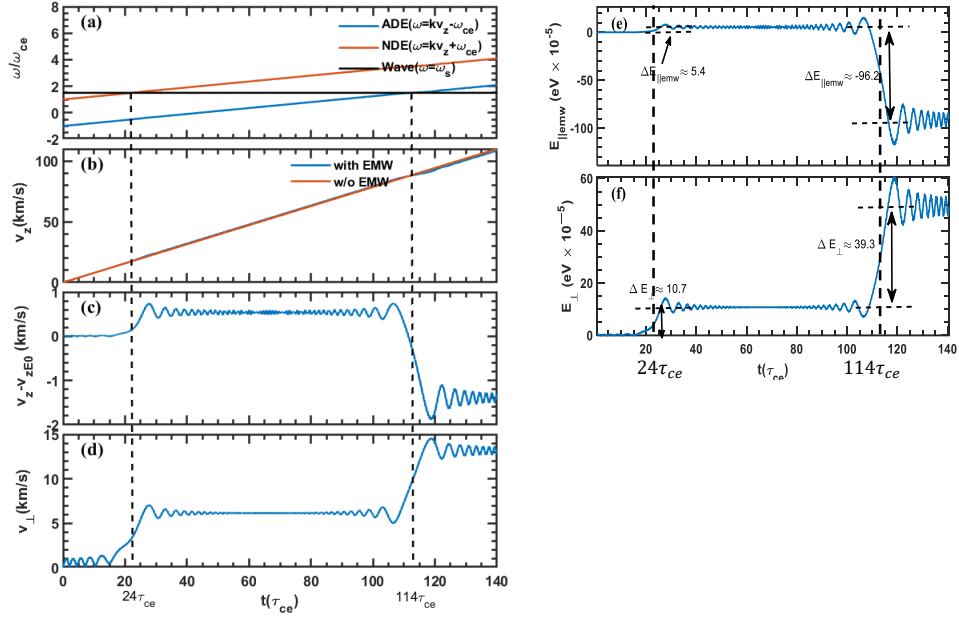
Fig. 5. Kinetic evolution of electrons in a magnetic field with an electromagnetic wave during acceleration. (a) Frequencies of ADE, NDE, and source wave frequency. (b) The parallel velocity v_z in the case with and without the electromagnetic wave. (c) The change of parallel velocity caused by the electromagnetic wave. (d) The cyclotron velocity $v_\perp$. (e) The parallel kinetic energy transferred to the electron by the electromagnetic wave. (f) The evolution of gyro-kinetic energy.

cyclotron system absorbing a photon during the NDR, resulting in an increase in both parallel kinetic energy and gyro-kinetic energy(internal energy). The change in parallel kinetic energy caused by the electromagnetic wave is shown in Fig. 5(e), where $\Delta T_{21} = \Delta E_{\parallel \text{emw}} \approx 5.4 \times 10^{-5}$ eV. The increase in gyro-kinetic energy is shown in Fig. 5(e), where $\Delta U_{21} = \Delta E_\perp \approx 10.7 \times 10^{-5}$ eV. The energy transfer ratio between internal energy and parallel kinetic energy during resonance is given by $\frac{\Delta U_{21}}{\Delta T_{21}} \approx 1.98$. According to quantum theory, the energy ratio is given by Eq. (13). Here $m = 1$ for NDE and $k = 10^5 \text{ m}^{-1}$ along the z-axis, the resonant velocity $v_z \approx 19 \times 10^3 \text{ m/s}$ and $\omega_{ce} \approx 3.51 \times 10^9 \text{ s}^{-1}$. Finally, $n_p = 1.85$, which is in close agreement with the simulation results.

The Anomalous Doppler Effect begins to emerge when the time reaches $113\tau_{ce}$, where $\omega_{\text{ADE}} = \omega$ as shown in Fig. 5(a). At this point, the parallel velocity begins to scatter into the perpendicular direction, evident from the decrease in Δv_z and the increase in $v_\perp$ as seen in Fig. 5(c) and Fig. 5(d). During the resonant period, the changes in parallel kinetic and gyro-kinetic energies caused by the electromagnetic wave are calculated as $\Delta T_{21} = \Delta E_{\parallel \text{emw}} \approx -96.2 \times 10^{-5}$ eV and $\Delta E_\perp \approx 39.3 \times 10^{-5}$ eV. The energy transfer ratio is $\frac{\Delta U_{21}}{\Delta T_{21}} \approx -0.408$. According to quantum theory, the change ratio of $\Delta U_{21}/\Delta T_{21} = -\hbar\omega_{ce}/\hbar\vec{k}\cdot\vec{v} = -0.3908$, where $\omega_{ce} \approx 3.51 \times 10^9 \text{ s}^{-1}$, and $k = 10^5 \text{ m}^{-1}$, $v_z = 90 \text{ km/s}$. The quantum theory results are in good agreement with the numerical calculations. The energy change ratio is also derived in the Appendix, based on classical theory.

3.3.Validation of the relationship with wave angular momentum.

Fig. 6(a–b) illustrate the velocity evolution under linear polarization of E_l, right-circular polarization E_R ($m = -1$), and left-circular polarization E_L ($m = 1$). The work done on the electron by the electromagnetic

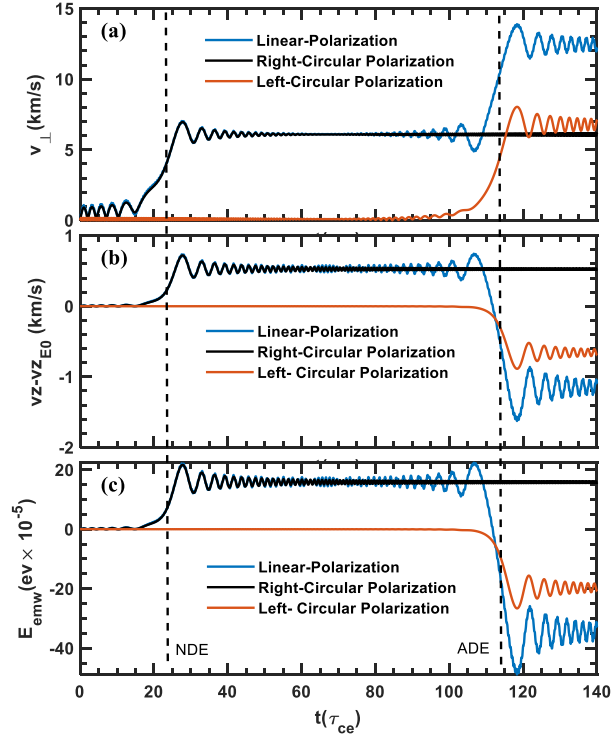Fig. 6. Velocity evolution caused by induced wave with linear, right-circular and left-circular polarization. (a) The cyclotron velocity $v_\perp$.(b) The change of parallel velocity caused by the electromagnetic wave.

wave, E_{emw}, as depicted in Fig. 6(c), consists of the parallel direction, $E_{\parallel\mathrm{emw}}$, as previously described, and the gyro-kinetic energy $E_{\perp\mathrm{emw}}$. The latter is calculated as $E_{\perp\mathrm{emw}} = \int \vec{F}_\perp \cdot \vec{v}_\perp \, dt$, where $\vec{F}_\perp$ is determined from the electric and magnetic field forces, and $\vec{v}_\perp$ represents the cyclotron velocity. All these parameters can be readily obtained from numerical results and integrated discretely.

The three types of polarization waves are investigated under the same scenario as before. As a result, the right-hand circularly polarized wave ($m = 1$) causes a velocity change only at around $23\tau_{ce}$, while the left-hand circularly polarized wave ($m = -1$) causes a velocity change only at around $113\tau_{ce}$. This indicates that the right-circularly polarized wave is responsible for the NDE, while the left-hand circularly polarized wave is responsible for the ADE, which agrees well with the quantum analysis.

For a left-circularly polarized (LCP) electromagnetic wave, The angular momentum selection rule ($m = -1$) restricts resonance to only occur when: $\omega = \vec{k} \cdot \vec{v} - \omega_{ce}$, as confirmed numerically in Fig. 7. This represents a significant departure from previous classical treatments [24] (Eqs. 36-37) that permitted resonance at arbitrary integer harmonics m, while being fully consistent with quantum angular momentum conservation principles.

4Discussion

Based on the momentum and angular momentum conservation analysis, we analyze the case where $\vec{k}$ is oriented opposite to $v_\parallel$(or $\vec{B}_0$). In this case, if a cyclotron electron emits a photon with left-hand circular polarization and momentum $-\hbar\vec{k}$, where the angular momentum carried by photon is $\hbar$, then after the emission, the change in internal energy is $\Delta U = -\hbar\omega_{ce} < 0$, and the change in translational kinetic energy $\Delta T = \hbar k v_\parallel > 0$.
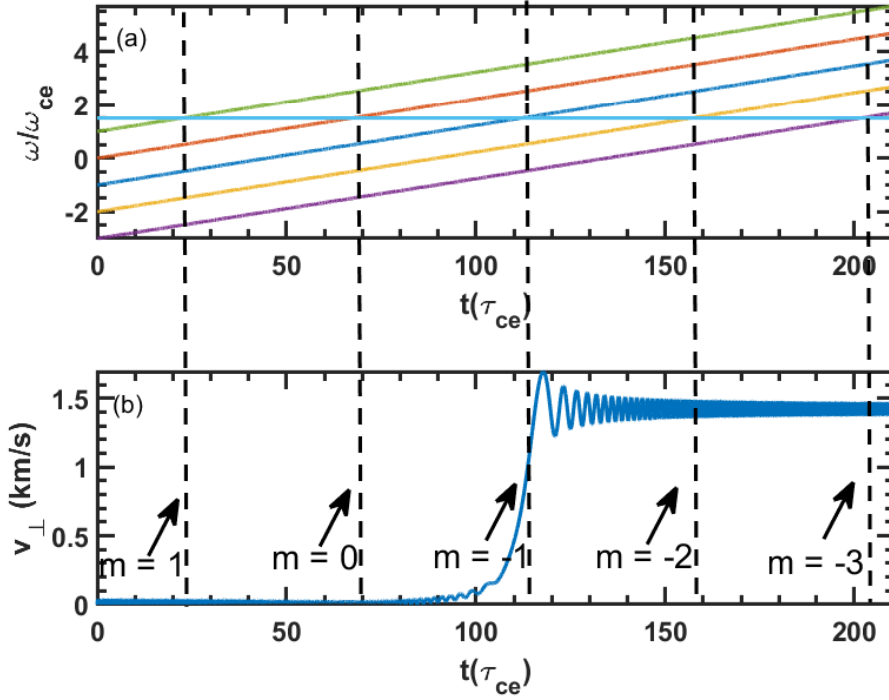
Fig. 7. (a) Frequency of $\omega = \vec{k} \cdot \vec{v} + m\omega_{ce}$ under different m values and induced wave frequencies.(b)Perpendicular velocity evolution under the left-circularly polarized wave, where $m = -1$.

However, if the emitting photon have right-circular polarization and momentum $-\hbar\vec{k}$, the change of internal energy becomes $\Delta U = \hbar\omega_{ce} > 0$, while the translational kinetic energy still is $\Delta T = \hbar k v_\parallel > 0$. This would violate the conservation of energy, as it is not possible for an electron to emit a photon while simultaneously increasing its total energy. Consequently, for a plane electromagnetic wave, only the left-circularly polarized component can resonate with an electron moving opposite to $v_\parallel$ (or $\vec{B}_0$).

The right-hand polarization case would violate energy conservation, as it requires the electron to emit a photon while simultaneously gaining total energy $(\Delta U + \Delta T > 0)$. Therefore, for a plane electromagnetic wave, only the left-circularly polarized component can resonantly interact with an electron moving antiparallel to $\vec{v}_\parallel$ while satisfying all conservation laws.

5.Conclusion

This paper presents a simple yet useful method to analyze the resonant process of NDE and ADE. The quantum method, combined with an angular momentum conservation analysis, illustrates that the parameter m in the resonant condition $\omega = \vec{k} \cdot \vec{v} + m\omega_{ce}$ is directly related to the angular momentum of the resonant wave. Numerical simulations based on the VPA method are also provided, confirming the correctness of the quantum results regarding both the angular momentum relationship between m and the energy transfer ratio.

Appendix A:Classical analysis of Anomalous Doppler Resonant

here we would like give a brief derivation of energy transformation through classical dynamic equation:

$$m_e \frac{d\vec{v}_\parallel}{dt} = -e(\vec{v}_\perp \times \vec{B}_\perp) \tag{19}$$

$$m_e \frac{d\vec{v}_\perp}{dt} = -e(\vec{v}_\perp \times \vec{B}_0 + \vec{v}_\parallel \times \vec{B}_\perp + \vec{v}_\perp \times \vec{B}_0) \tag{20}$$

Consider $\vec{B}_\perp = \frac{\vec{e}_k \times \vec{E}_\perp}{v_p}$, where $\vec{e}_k$ is the unit vector of wave vector of E.M. wave, which is along the z-axis. Using $\vec{v}_\parallel$ and $\vec{v}_\perp$ to dot both sides of (19) and (20), substitute $\vec{B}_\perp$ and simplify the equations, we have

$$m_e \vec{v}_\parallel \cdot \frac{d\vec{v}_\parallel}{dt} = -e(\vec{v}_\perp \cdot \vec{E}_\perp) \frac{v_\parallel}{v_p} \tag{21}$$

$$m_e \vec{v}_\perp \cdot \frac{d\vec{v}_\perp}{dt} = e(\vec{v}_\perp \cdot \vec{E}_\perp) \frac{v_\parallel}{v_p} - e(\vec{v}_\perp \cdot \vec{E}_\perp) \tag{22}$$

Here $v_p = \frac{\omega}{\kappa}$, the total energy change of electron can be expressed as:

$$\frac{d}{dt} \left(\frac{1}{2} m_e v_\parallel^2 + \frac{1}{2} m_e v_\perp^2 \right) = -e(\vec{v}_\perp \cdot \vec{E}_\perp) \tag{23}$$

The sign of $-e(\vec{v}_\perp \cdot \vec{E}_\perp)$ determines whether the electromagnetic (E.M.) wave undergoes "emission" ($-e(\vec{v}_\perp \cdot \vec{E}_\perp) < 0$) or "absorption" ($-e(\vec{v}_\perp \cdot \vec{E}_\perp) > 0$) of E.M. wave, and this is dependent on the phase difference between $v_\perp$ and $E_\perp$.

From (22) we have

$$e(\vec{v}_\perp \cdot \vec{E}_\perp) = \frac{m_e \vec{v}_\perp \cdot \frac{d\vec{v}_\perp}{dt}}{v_\parallel - 1} \tag{24}$$

Substitute (24) into (21), we have

$$m_e \vec{v}_\parallel \cdot \frac{d\vec{v}_\parallel}{dt} = -\frac{m_e \vec{v}_\perp \cdot \frac{d\vec{v}_\perp}{dt}}{v_\parallel - 1} \frac{v_\parallel}{v_p} \tag{25}$$

Integrate (25), we have

$$\frac{1}{2} m_\rho \left(v_1 - \frac{\omega}{k} \right)^2 + \frac{1}{2} m_\rho v_\perp^2 = C_0 \tag{26}$$

Here C_0 refers to the initial value. The change in velocity is constrained to a circular trajectory, as shown in Fig. 8. At the normal Doppler resonance (NDR), where $v_1 = \frac{\omega - \omega_{ce}}{k}$, an increase in v_1 corresponds to an increase in $v_\perp$. In contrast, at the anomalous Doppler resonance (ADR), where $v_\parallel = \frac{\omega + \omega_{ce}}{k}$, an increase in $v_\parallel$ corresponds to a decrease in $v_\perp$.

The change of energy in translational energy and gyro-kinetic energy can be written as follows:

$$\frac{\Delta U}{\Delta T} = \frac{v_\perp d v_\perp}{v_\parallel d v_\parallel} \tag{27}$$

From (26), we have

$$\frac{d v_\perp}{d v_\parallel} = -\frac{v_\parallel - \frac{\omega}{k}}{v_\perp} \tag{28}$$
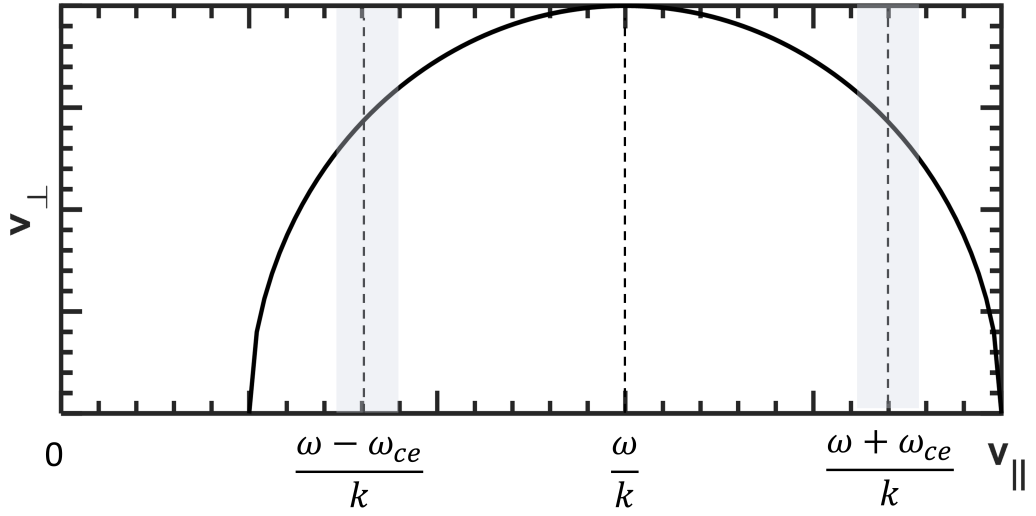
Combining (27) and (28), we have

Fig. 8. The trajectory curve of $(v_{\parallel}, v_{\perp})$.

$$\frac{\Delta U}{\Delta T} = -\frac{v_{\parallel} - \frac{\omega}{k}}{v_{\parallel}} \qquad (29)$$

According to the resonant condition $\omega = k v_{\parallel} + m \omega_{ce}$, substituting $v_{\parallel}$ with ω and k in (29), we obtain:

$$\frac{\Delta U}{\Delta T} = \frac{m \omega_{ce}}{k v_{\parallel}} \qquad (30)$$

which agrees with the quantum result as Eq. refeq:DU21DT21.

References

[1] Tamm I E 1959 Nobel Lectures 18 122–133

[2] Frank I 1960 Science 131 702–712

[3] Ginzburg V L 1960 Soviet Physics Uspekhi 2 874

[4] Shustin E, POPOVICH P and Kharchenko I 1971 SOVIET PHYSICS JETP 32

[5] Ginzburg V and Frank I 1946 Journ. of Experimental and Theoretical Physics (JETP) V 16 15–26

[6] Nezlin M V 1976 Soviet Physics Uspekhi 19 946

[7] Santini F, Barbato E, De Marco F, Podda S and Tuccillo A 1984 Physical review letters 52 1300

[8] Kho T and Lin A 1988 Physical Review A 38 2883

[9] Wang Y, Qin H and Liu J 2016 Physics of Plasmas 23

[10] Guo Z, McDevitt C J and Tang X Z 2018 Physics of Plasmas 25

[11] Liu C, Hirvijoki E, Fu G Y, Brennan D P, Bhattacharjee A and Paz-Soldan C 2018 Physical Review Letters 120 265001

[12] Shi X, Lin X, Kaminer I, Gao F, Yang Z, Joannopoulos J D, Soljačić M and Zhang B 2018 Nature Physics 14 1001–1005

[13] Filatov L and Melnikov V 2021 Geomagnetism and Aeronomy 61 1183–1188

[14] Artsimovich L, Bobrovskii G, Mirnov S, Razumova K and Strelkov V 1967 Soviet Atomic Energy 22 325–331

[15] Kadomtsev B and Pogutse O 1968 Sov. Phys. JETP 26 1146–1150

[16] Spong D A, Heidbrink W, Paz-Soldan C, Du X, Thome K, Van Zeeland M, Collins C, Lvovskiy A, Moyer R, Austin M et al. 2018 Physical Review Letters 120 155002

[17] Liu Y, Zhou T, Hu Y, Liu C, Zhou R, Zhang T, Zhao H, Zhu Z, Liu X and Ling B 2019 Nuclear Fusion 59 106024

[18] Gorozhanin D, Ivanov B, Khoruzhiy V, Onishchenko I and Miroshnichenko V 1997

[19] Sajjad S et al. 2007 Chinese Physics Letters 24 3195

[20] Castejon F and Eguilior S 2003 Particle dynamics under quasi-linear interaction with electromagnetic waves Tech. rep. Centro de Investigaciones Energeticas

[21] Zhang Q, Zhang Y, Tang Q and Tang X Z 2024 arXiv preprint arXiv:2409.15830

[22] Ginzburg N 1979 Radiophysics and Quantum Electronics 22 323–330

[23] Coppi B, Pegoraro F, Pozzoli R and Rewoldt G 1976 Nuclear Fusion 16 309

[24] Dendy R 1987 The Physics of fluids 30 2438–2441

[25] Ginzburg V 2005 Acoustical Physics 51 11–23

[26] Frolov V and Ginzburg V 1986 Physics Letters A 116 423–426

[27] Ginzburg V L 1996 Physics-Uspekhi 39 973

[28] Arnaut H and Barbosa G 2000 Physical review letters 85 286

[29] Kiang D and Young K 2008 American Journal of Physics 76 1012–1014

[30] Wei E, Lan Z, Chen M L, Chen Y P and Sun S 2024 IEEE Journal on Multiscale and Multiphysics Computational Techniques

[31] Liu H, He X, Chen S and Zhang W 2004 arXiv preprint physics/0411183

[32] Qian B L 1999 IEEE transactions on plasma science 27 1578–1581

[33] Weyssow B 1990 Journal of plasma physics 43 119–139

[34] Gogoberidze G and Machabeli G 2005 Monthly Notices of the Royal Astronomical Society 364 1363–1366

[35] Roberts C S and Buchsbaum S 1964 Physical Review 135 A381

[36] Bourdier A and Gond S 2000 Physical Review E 62 4189

[37] Nusinovich G S, Korol M and Jerby E 1999 Physical Review E 59 2311

[38] Nusinovich G S, Latham P and Dumbrajs O 1995 Physical Review E 52 998

[39] Qian B L 2000 Physics of Plasmas 7 537–543

[40] Zhang R, Liu J, Qin H, Wang Y, He Y and Sun Y 2015 Physics of Plasmas 22